Chemistry & Biology, Vol. 12, 895–904, August, 2005, ©2005 Elsevier Ltd All rights reserved. DOI 10.1016/j.chembiol.2005.05.020

Microbial Enzymes Mined from the Urania Deep-Sea Hypersaline Anoxic Basin

Manuel Ferrer,[1,2,*] Olga V. Golyshina,[1] Tatyana N. Chernikova,[1] Amit N. Khachane,[1] Vitor A.P. Martins dos Santos,[1] Michail M. Yakimov,[3] Kenneth N. Timmis,[1,4] and Peter N. Golyshin[1,4]

[1]Department of Microbiology
GBF—German Research Centre for Biotechnology
38124 Braunschweig
Germany

[2]Institute of Catalysis
CSIC
Cantoblanco
28049 Madrid
Spain

[3]Istituto per l'Ambiente Marino Costiero
CNR
98100 Messina
Italy

[4]Institute of Microbiology
Technical University Braunschweig
38124 Braunschweig
Germany

Summary

We created a metagenome expression library from the brine:seawater interface of the Urania hypersaline basin, screened it for esterases, and characterized five of these. Two had no significant sequence homology to known esterases, hydrolyzed both carboxylesters and thioesters, and exhibited unusual, habitat-specific characteristics (preference for high hydrostatic pressure and salinity). One has an unusual structural signature incorporating three catalytic active centers mediating distinct hydrolytic activities and an adaptive tertiary-quaternary structure that alters between three molecular states, according to the prevailing physicochemical conditions. Some of the esterases have high activities, specificities, enantioselectivities, and exceptional stability in polar solvents, and they are therefore potentially useful for industrial biotransformations. One possesses the highest enantioselectivity toward an ester of the important chiral synthon solketal (*E*: 126[S]; 98%*ee*).

Introduction

One of the most exciting current research endeavors is the exploration of biological and functional diversity, especially that existing in the extreme conditions that can occur at the limits of the biosphere [1–5]. This will not only lead to discovery of unknown metabolic and physiological activities and molecular and cellular structures, and reveal the range of potential life forms on Planet Earth, but also enable definition of the mechanistic basis of life under the most hostile conditions at the extremities of the biosphere. Moreover, there is a pervasive perception that undiscovered microbial diversity is enormous and is a treasure trove for new biotechnological applications [6–9]. Defining the limits of metabolic diversity and microbial lifestyles on Planet Earth will provide a tangible framework for the development of new applications for the future.

Deep-sea hypersaline anoxic basins of the Eastern Mediterranean (DHABs) (Figure 1) represent unique, extreme, and largely unexplored habitats, >3500 m below sea level, which were created 5–6 million years ago by the dissolution of buried Messinian evaporitic deposits to form very stable brines entrapped in sea floor basins and sharply stratified from the overlying water column [10–13]. They are characterized by extremely high salinity and corresponding density, high hydrostatic pressure, absence of light, anoxia, and a sharp chemocline (see Figures S1 and S2 in the Supplemental Data available with this article online). These physicochemical features have ensured that the DHABs have been physically isolated from other habitats on the planet for thousands (2,000–176,000) of years [14, 15], may have resulted in the selection of unusual organisms, and probably prevented their dispersal; therefore, they are expected to yield novel microbial diversity and unknown cellular gene products with interesting properties. In this study, we have posed the question: Is new enzymatic diversity, exemplified by esterases, to be found in microbes present in DHABs, specifically in the brine:seawater interface of the Urania West Basin, one of five recently discovered DHABs in the Southeastern Mediterranean Sea (the others being the Bannock, Atalante, Discovery, and Tyro Basins)? The results we report here, obtained by generating and screening a metagenome expression library, document the discovery of five esterases, two of which function under the extreme conditions of DHAB brines, and a one of which possesses an adaptive structure:function configuration that confers high catalytic activities under a very wide range of physicochemical conditions. They also demonstrate that DHAB esterases are promising candidates for the synthesis of optically pure biological active substances that provide access to pharmaceutical intermediates.

Results

Esterases Yielded by Urania DHAB Interface

DHABs represent isolated, extreme environments that harbor thus far uncharacterized biodiversity [13]. To explore the functional biodiversity of the seawater:brine interface of one such DHAB, the Urania West Basin was sampled during the BIODEEP-II cruise of the RV *Urania* in September, 2001, and a subsample was immediately supplemented with sterile crude oil (Arabian Light, 0.5% v/v) to stimulate microbial growth and increase biomass. After incubation for 4 weeks at 15°C, total DNA was extracted from the culture, and a metagenome expression library in *Escherichia coli* was generated by using the bacteriophage lambda-based ZAP

*Correspondence: mferrer@icp.csic.es

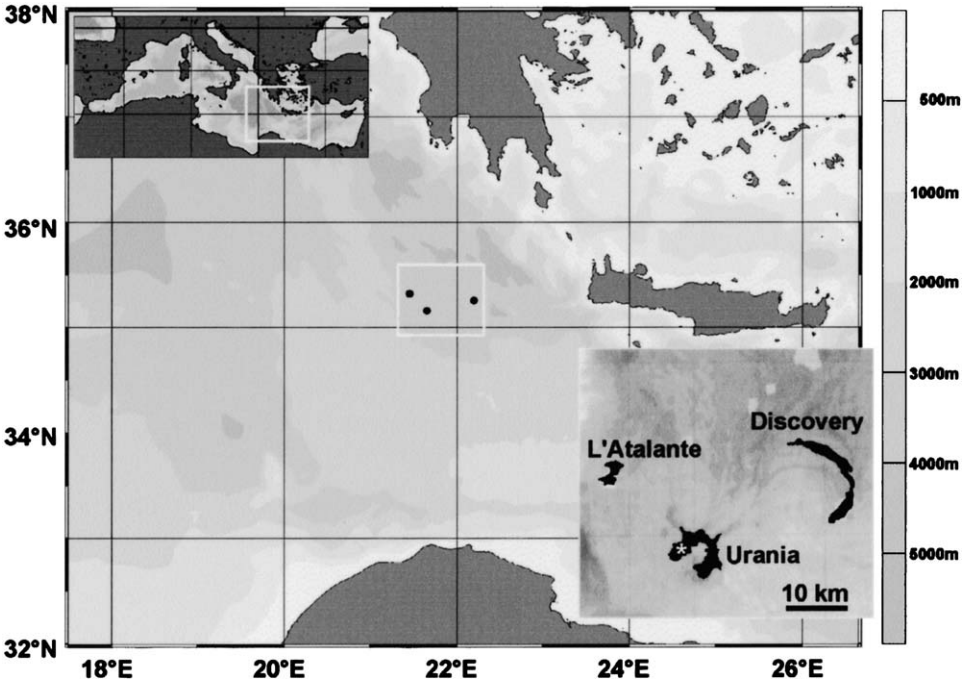

Figure 1. Location of Three Deep Anoxic Hypersaline Basins in the Eastern Mediterranean Sea

The map was constructed with Ocean Data View software [31]. The detailed map of basin profiles is shown in the inset map (bottom right). The sampling site (35°13′51′′N; 21°28′24′′E; 3552 m depth) is shown by a white asterisk.

phagemid vector (Stratagene), as described in Experimental Procedures. Part of the library was screened for esterase activity, and five phagemids, designated pBKOil2, pBKO.02, pBKO.16, pBKO.21, and pBKO.23 were identified as esterase-positive and were sequenced. Their esterase genes were subsequently expressed in *E. coli* XLOLR, and the enzymes were purified and N-terminally sequenced to confirm the gene assignments.

The Oil2, O.02, O.16, O.21, and O.23 esterase genes specified polypeptides that were 202, 515, 913, 313, and 519 amino acids long, with predicted sizes of 22,044, 55,771, 104,369, 35,616 and 44,444 Da and isoelectric points of 5.36, 4.96, 4.57, 4.90, and 5.03, respectively. Multiple sequence alignments and phylogenetic analysis for all esterase-like sequences were performed with the online ClustalW tool (http://www.ebi.ac.uk) and MacVector 7.2.2 software (Accelrys, San Diego, CA) with BLOSUM matrix (see Figure S3). No convincing indications of signal peptide sequences of excreted proteins were found for any enzyme when using the SignalP and Sigcleave tools. The Oil2 carboxylesterase (e value better than e^{-33}; identity ranging from 43% to 51%) belongs to the ester hydrolase family IV of the Arpigny and Jaeger classification, based on the conserved motifs surrounding the catalytic residues of family IV (/GDSAGG/, /DPL/, /HGF/) (Figures S3A–S3C) [16]. According to sequence alignments, Ser40 and His173 residues belong to the catalytic triad; however, an aspartic acid typical of serine hydrolases [16] is lacking. The O.02 (e value better than e^{-28}; 43%–51% identity) and O.23 (e value better than e^{-28}; 30%–42% identity) enzymes also contain the GXSXG motif and returned similar sequences as BLAST hits, although unusual motifs surrounding the catalytic serine residue, and a lack of a conserved histidine residue of the catalytic triad, suggest that they represent a new family of serine hydrolases (Figures S3D–S3H). Interestingly, the O.16 and O.21 esterases showed no convincing BlastP hits in the SwissProt/TREMBL and NCBInr databases. A search of the Pfam database (http://www.sanger.ac.uk/Software/Pfam/) for possible conserved domains of the O.16 enzyme revealed three potential lipase family motifs (two GXSXG [/GTSSG/ and /GGSNG/] and one GDS(L) [/GDS/]), a possibility supported by analysis with 3D-PSSM, a tool based on a threading algorithm, which also assigned them to the "α/β fold protein" class, and to the "esterase/acetylhydrolase" superfamily, with the PSSM e value of 0.0043 (Figures S3I and S3J). Although, none of these motifs was found in the O.21 esterase sequence, alignments suggest that Ser200, Asp344, and His347 may form the catalytic triad (Figures S3K and S3L).

Esterases Exhibit Habitat-Specific Characteristics

To investigate whether the DHAB esterases exhibited habitat-specific features, the DHAB esterase genes were expressed in *E. coli*, and their products were purified and characterized.

Subunit Compositions

The subunit structures of the purified esterases were deduced from the ratios of the experimentally determined molecular weights of the undenatured proteins (assessed by polyacrylamide gel electrophoresis and

gel filtration) and from their subunit molecular weights, which were determined by translation of their gene sequences. According to that, the enzymes were found to be either monomeric, in which esterases were specified by O.02 (57,600:55,771 Da), O.16 (104,000:104,369 Da), O.21 (40,800:35,616 Da), and O.23 (45,000:44,444 Da), or dimeric, in which the esterase is specified by Oil2 (44,500:22,044 Da).

Acyl Chain Specificities

The acyl chain length specificities of DHAB enzymes were estimated by using short chain (C_2–C_6), medium chain (C_8–C_{12}), and long chain (C_{14}–C_{18}) *p*-nitrophenyl esters (*p*-NP-esters) and triglycerols (Table S1). Maximal hydrolytic rates were obtained with the C_2 (for O.16 and O.21 enzymes), C_3 (for O.02 and O.23 enzymes), or C_4 (for Oil2 enzyme) *p*-NP-esters, with specific activities ranging from 225–4500 U/mg protein. All five DHAB esterases hydrolyzed short chain triacylglycerols such as triacetin (141–651 U/mg protein), whereas only one, O.16, hydrolyzed tripropionin (268 U/mg protein). The activity declined with longer chain length esters, which suggests that the enzymes were esterases rather than lipases. Maximum specific activity values were measured with O.23 and Oil2 (4200–4500 U/mg), followed by O.21 and O.02 (2500–3000 U/mg), and finally O.16 (573 U/mg).

pH and Temperature Optima

The pH optima of the purified esterases using *p*-NP-esters ranged from 8.0 (O.02 and O.23 enzymes) to 8.5 (O.21 and Oil2 enzymes) and 9.0 (O.16 enzyme). The O.16 esterase retained 80% of its activity at pH 12.0. The temperature optima were 40°C for the Oil2 enzyme, 50°C for the O.16 and O.23 enzymes, and 60°C for the O.02 and O.21 enzymes. O.02, O.16, O.21, O.23, and Oil2 esterases were significantly stable ($t_{1/2}$ > 600 min) at temperatures of 67°C, 59°C, 59°C, 53°C, and 48°C and pHs of 10.0, 12.0, 11.0, 10.0, and 10.0, respectively (Table S2).

Influence of Cations

Although most cations did not have major effects on the esterases, Na^+ and/or K^+ ions strongly stimulated the activity of three enzymes and mildly stimulated one (Figure 2A): 2–4 M NaCl elicited a 180× increase in the activity of the O.16 enzyme (from 600 to 103,000 U/mg protein); 3.5 M NaCl caused a 40× increase in the activity of the O.21 enzyme (from 3000 to 117,000 U/mg protein), and a 30× increase in the activity of the Oil2 enzyme (from 4170 to 125,100 U/mg protein); and 25–75 mM NaCl induced a 2.4× increase in the activity of the O.23 enzyme (from 4,500 to 10,800 U/mg protein). In contrast, the O.02 enzyme was significantly inhibited (from 2460 to 96 U/mg protein) at concentrations >25 mM of Na^+K^+ and Na^+ ions stimulated or inhibited to similar extents.

Effect of Hydrostatic Pressure

Given the high pressure prevailing at the DHABs, ca. 40 MPa (see [13]), we also investigated the activity:hydrostatic pressure relationships of DHAB esterases by assaying the enzymes after exposure to different pressures (0–40 MPa) for 60 min (Figure 2B). While increasing pressures progressively inactivated the Oil2, O.02, and O.23 esterases (54%–62% residual activity after exposure to 40 MPa), the effect on the O.21 esterase was insignificant (>95% activity retained after exposure to 40 MPa). Moreover, the activity of the O.16 enzyme (measured with *p*-NP-butyrate as a substrate) increased with increasing pressure to a maximum at ~20 MPa (1.9× more active than at atmospheric pressure: 1089 versus 573 U/mg protein), and it was still 1.5× more active after exposure to 40 MPa (861 versus 573 U/mg protein). Increased hydrostatic pressure applied for 1 hr or 24 hr had essentially the same effect on enzymatic activity. The presence or absence of Na^+ did not influence the activity:hydrostatic pressure relationship.

Influence of Solvents

All esterases were active and stable in nonpolar and medium polar solvents, like hexane, isooctane, toluene, and *t*-butylalcohol (data not shown), which are used in a variety of biotransformations [17]. In addition, some were also highly active in, and even stimulated by, polar solvents like *n*-propanol, ethanol, and dimethylsulfoxide (Figure 2C; Figure S4). The O.16 esterase was the most active and stable of all and was 2× more active in the presence of 70% (v/v) ethanol or *n*-propanol (1333 versus 573 U/mg protein, with *p*-NP-butyrate).

Inactivation by Active Site Inhibitors

To probe residues involved in catalysis, the esterases were incubated with various inhibitors, and their hydrolytic activities were subsequently determined. The active center inhibitors phenylmethyl sulfonylfluoride, dodecyl sulfonylchloride, diisopropyl fluorylphosphate, and diethyl pyrocarbonate inhibited all of the esterases (IC_{50} values ranging from 10 to 83 μM), suggesting involvement of serine residues at the active sites. The O.16 enzyme was stimulated 2-fold by cysteine-specific reagents like N-ethylmaleimide, iodoacetate, *p*-chloromercuribenzoate (CMB), *p*-chloromercuriphenylsulphonic acid (PCMPS), dithiotreitol (DTT), and 2-mercaptoethanol, whereas the Oil2, O.02, O.21, and O.23 enzymes were inhibited (K_i values [average] of 1.5 ± 0.04, 3.2 ± 0.09, 7.4 ± 0.14, and 6.5 ± 0.12 μM, respectively [pH 8.5]). The Oil2, O.16, and O.23 enzymes were strongly inhibited by histidine-specific inhibitors such as tosylphenylalanylchloromethane (PCK) and diethyl pyrocarbonate (DEPC) (K_i values [average] of 3.5 ± 0.08, 7.4 ± 0.14, and 5.9 ± 0.11 μM, respectively [pH 8.5]), indicating that histidine residues are probably involved in the catalytic function of the enzymes. However, none of these chemicals inhibited the O.02 and O.23 enzymes, suggesting that histidine residues are not involved in catalysis [18].

Kinetic Characterization of DHAB Esterases

The kinetic parameter K_m, k_{cat}, and k_{cat}/K_m values of the esterases were estimated with a series of 26 commonly used ester substrates in the concentration range of 0–50 mM, at optimal salt concentrations (Table S3). The kinetics parameters derived by a Lineweaver-Burk plot showed that, among the *p*-NP-esters examined, *p*-NP-butyrate was the preferable substrate for Oil2, *p*-NP-propionate was preferable for O.02 and O.23, and *p*-NP-acetate was preferable for O.16 and O.21. As the chain length of the substrate increased, the specificity constant k_{cat}/K_m decreased, though with little effect on K_m. The most efficient esterases in the hydrolysis of *p*-NP-esters were Oil2, O.16, and O.21 (k_{cat}/K_m = 3500–3900 $s^{-1}mM^{-1}$), followed by O.02 and O.23 (113

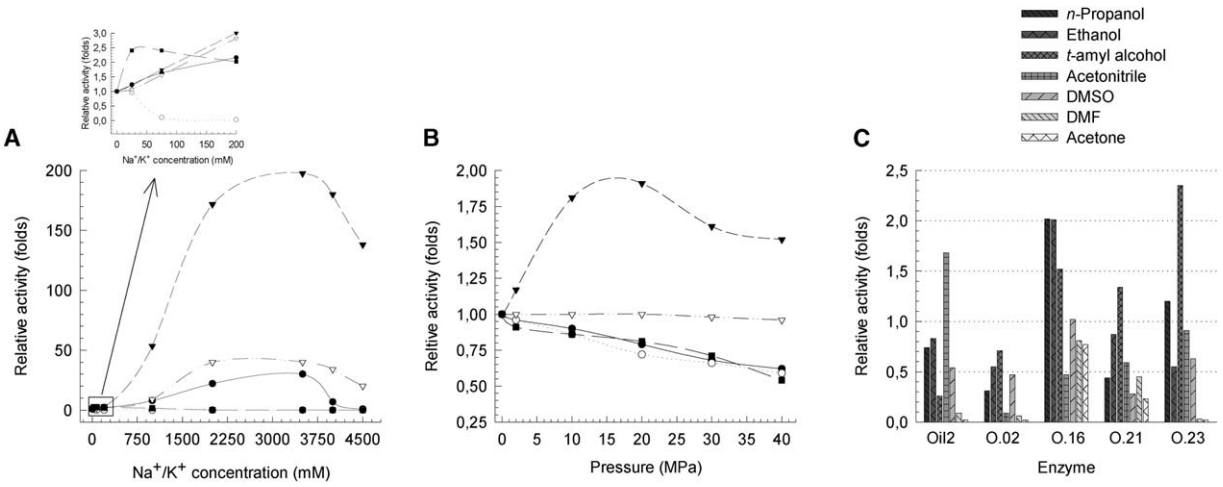

Figure 2. Parameters Affecting Activity of DHAB Esterases

(A) Effect of Na^+ on esterase activity. Activation or depression of esterase activity by K^+ was similar to that found with Na^+ (6% variation). The inset shows the area ranging from 0 to 200 mM Na^+ magnified.

(B) Effect of pressure on esterase activity.

(C) Effect of solvents on esterase activity.

Esterase activity was measured by using the standard assays described in the Supplemental Data. Reaction conditions: [E] = 5 μg, [substrate] = 0.8 mM for *p*-NP-esters; 100 mM Tris-HCl (pH 8.5); *T* = 40°C. All values were determined in triplicate and were corrected by considering the spontaneous hydrolysis of the substrate. Activation levels in (B) and (C) are expressed as a percentage of the control value obtained without addition of organic solvent or in samples not subjected to pressure. Activity values corresponding to 302 (for Oil2), 1385 (for O.02), 573 (for O.16), 2916 (for O.21), and 225 (for O.23) U/mg protein were taken as 1.

and 404 $s^{-1}mM^{-1}$, respectively). The K_m values for triacetin and tripropionin were similar to those of *p*-NP-esters, although all the enzymes were 30-fold less efficient with these substrates (k_{cat}/K_m values varied between 41 and 2800 $s^{-1}mM^{-1}$). O.16 and O.21 also hydrolyzed propionyl coenzyme A (propionyl-CoA) (K_m = 0.13–0.33 mM; k_{cat}/K_m = 1200–1400 $s^{-1}mM^{-1}$) and phenylacetyl-CoA (K_m = 1.60 mM; k_{cat}/K_m = 75 $s^{-1}mM^{-1}$), and thus exhibited acyl-coenzyme A thioesterase activities. One of the five DHAB enzymes, O.16, was also able to hydrolyze esters of 4-hydroxybenzoic acid (parabens) and their analogs, with the highest preference for propyl paraben (678 $s^{-1}mM^{-1}$), followed by that for methyl paraben (174 $s^{-1}mM^{-1}$; the value for methyl 3-hydroxybenzoate was nearly as high, 263 $s^{-1}mM^{-1}$), butyl paraben (65 $s^{-1}mM^{-1}$), and methyl benzoate (13 $s^{-1}mM^{-1}$). Methyl 2-hydroxybenzoate was poorly hydrolyzed (0.6 $s^{-1}mM^{-1}$). The K_m values for hydroxybenzoate esters were in the range of 0.9 (for propyl paraben)–8.0 mM (for methyl 2-hydroxybenzoate). Substrates with an α amino group, such as D-phenylglycine amide and D-phenylglycine methyl ester, were also good substrates for the O.21 enzyme (K_m = 0.6–0.7 mM; k_{cat} = 243–267 s^{-1}; k_{cat}/K_m = 347–445 $s^{-1}mM^{-1}$), though analogs like phenylacetic acid methylester lacking the α amino group were not hydrolyzed. These substrate specificities suggest that the O.16 and O.21 esterases are exceptional multifunctional enzymes acting on an unusual combination of substrates, whereas the Oil2, O.02, and O.23 esterases are more conventional and act on the most common esterase substrates. Moreover, although the K_m values for the substrates assayed (from 0.1 to 8.0 mM) were in the same range as those of other esterases and lipases, the k_{cat}/K_m ratios of three of the five esterases greatly exceed published values for the hydrolysis of *p*-NP-esters, paraben analogs, and α amino acid esters (600–3900 versus 400 $s^{-1}mM^{-1}$).

Enantioselectivity of DHAB Esterases

We employed the Quick E colorimetric assay [19] to analyze the enantioselectivity of DHAB esterases. First, we screened them with a variety of racemic esters to eliminate hydrolases that did not catalyze the hydrolysis of either enantiomer (Table S4). This screen identified O.16 and O.21 as the most active hydrolases of important racemic substances (specific activities: from 240 to 18,000 U/mg). We then estimated the enantioselectivity (E_{app}) of the five hydrolases by separate measurements of the initial rates of hydrolysis of each enantiomer by using the Quick E assay (see the Supplemental Data). It should be mentioned that the ratios obtained by these measurements were not true enantiomeric ratios (E_{true}), because the rates of hydrolysis of the enantiomers were measured separately; nevertheless, recent studies have clearly demonstrated that apparent (E_{app}) and true (E_{true}) enantioselectivity values closely match each other [20]. All DHAB esterases exhibited good enantiomeric ratios (E_{app} values of 20–117; Table 1), although enantio-preferences varied with enzyme and substrate. The O.16 esterase hydrolyzed solketal acetate, whose hydrolysis product is an important building block for the synthesis of pharmaceuticals, including anti-AIDS drugs and other biologically active compounds [19, 21], with an E_{app} value of ~64 with S-stereo-preference, which greatly exceeds the

Table 1. Estimated Apparent Enantioselectivities of DHAB Esterases toward a Variety of Chiral Esters

	Enantiomeric Ratio, E_{app} [Stereo-Preference][a]				
Substrate	Oil2	O.02	O.16	O.21	O.23
Solketal acetate	1.1 [R]	14.4 [R]	64.0 [S]	8.6 [S]	5.6 [R]
2-methyl-glycidyl	2.2 [R]	9.8 [R]	2.7 [S]	25.5 [S]	39.8 [R]
1-phenyl acetate	1.1 [R]	42.8 [R]	116.2 [S]	29.7 [S]	9.2 [R]
Menthyl acetate	21.0 [R]	27.6 [R]	39.9 [S]	39.5 [S]	21.5 [R]
Methyl 3-hydroxybutyrate	—[b]	1.3 [R]	25 [S]	6.5 [S]	3.1 [R]
Pantolactone	—	11.0 [R]	—	8.3 [S]	4.4 [S]
Dihydro-5-hydroxymethyl-2(3H)-furanone	—	—	—	55.0 [S]	5.9 [S]
Methyl-3-bromo-2-methylpropionate	14 [S]	84.2 [R]	114 [S]	65.8 [R]	18.6 [R]
Methyl-3-hydroxy-2-methylpropionate	24 [R]	29 [R]	2.9 [R]	9.9 [S]	9.3 [R]
Alanine methyl ester	—	7.6 [S]	—	29.8 [S]	8.8 [R]
Tryptophan methyl ester	—	3.7 [R]	—	20.0 [S]	4.6 [S]
Methyl lactate	5.2 [R]	96 [S]	39.5 [R]	19.3 [S]	2.6 [S]
N-benzyl ethyl ester	3.8 [R]	3.7 [R]	59.6 [S]	21.5 [R]	2.8 [R]
Methyl 2,2-dimethyl-1,3-dioxane-4-carboxylate	—	—	59.0 [S]	10.4 [S]	—
Ketoprofen methyl ester	—	—	53 [R]	—	35 [R]

[a] All measurements were performed three times under the following conditions: 96-well microtiter plates containing 5 μg pure protein, 10 mM substrate, 0.8 mM resorufin acetate as internal standard, and 0.911 mM phenol red, all in 200 μl 5 mM EPPS buffer (*N*-(2-hydroxyethyl)piperazine-*N*′-(3-propanesulfonic acid) [pH 8.0]) per well; monitored colorimetrically at 550 nm. Hydrolytic activities were measured at 40°C in the presence of the optimum concentration of Na^+ ions (4 M NaCl for the Oil16 enzyme, 3.5 M NaCl for the Oil2 and O.21 enzymes, 25 mM NaCl for the O.23 enzyme, and no supplement for the O.02 enzyme). Apparent enantiomeric ratios for each substrate and enzyme pair were performed as described by Janes et al. [7].
[b] No hydrolysis product detected.

best values published so far for this substrate (14.8 for horse liver esterase [21] and 9.0 for *Burkholderia cepacia* lipase [22]). This value has been verified by the conventional endpoint method [23] in small scale-up reactions by using gas chromatography to measure the enantiomeric purity (Table 2). Under conditions similar to those used in the screening procedures, the E_{app} values agreed with the endpoint E_{true} within a factor of 2.4: the Quick E assay underestimated the true enantioselectivity for the hydrolysis of (R,S)-solketal acetate, which was calculated to be ~126 ± 2.4[S] (~98%*ee*) for the O.16 esterase, which was the most selective hydrolase.

Transesterification Activities of the O.16 and O.23 Enzymes

As shown in Figure S5A, the O.16 enzyme was able to carry out efficient transesterification of propyl paraben in the presence of 5% (v/v) methanol. The yield of methyl paraben after 160 min was 96% (initial amount of propyl paraben in solution: 0.5 mM), with 4% of the side product *p*-hydroxybenzoic acid. The O.21 esterase was able to catalyze the synthesis of esters with an α amino group—for example, the synthesis of ampicillin from D-phenylglycine methylester (80 mM) and 6-amino penicillanic acid (6-APA) (60 mM)—with a conversion of 66% after 2.5 hr, without appreciable hydrolysis of the transesterification product (Figure S5B).

O.16 Esterase, a Multicatalytic Site, Bifunctional Enzyme that Exhibits an Adaptive Tertiary/Quaternary Structure

Characterization of the O.16 esterase revealed that it exhibits exceptional activity and stability under the extreme environmental conditions characterizing the DHABs, namely, high salt, high pressure, and low redox potential. Three distinct active forms of the purified enzyme were detected (Figure S6). Under standard conditions (corresponding to those obtained in the upper water column), it exists as a monomeric protein of ~104 kDa (N-terminal sequence: LNNSGYTAAQWAAINSGITQ). In the presence of the reducing agent dithiotreitol (DTT), it dissociated into two active polypeptide species of 85 and 21 kDa, having N-terminal sequences of LNNSGY TAAQWAAI and MYGLPTVVMG, corresponding to amino acid residues 1–14 and 771–780, respectively, of the translated sequence of the O.16 esterase gene. This indicates that the primary translation product of the O.16

Table 2. True Enantioselectivity of DHAB Esterases Toward (R,S)-Solketal Acetate Measured by the Endpoint Method

Hydrolase	Reaction Time (hr)	ee_S [%][a]	ee_P [%][a]	C [%][b]	True E[c]	Estimated E[d]	Stereo-Preference
Oil2	7.0	18.0	38.3	31.9	2.6 ± 0.1	1.1	R
O.02	6.5	40.0	82.0	32.7	15.2 ± 1.0	14.4	R
O.16	3.9	38.0	98.0	28.0	125.6 ± 2.4	64.0	S
O.21	4.1	25.0	81.6	23.5	12.4 ± 0.9	8.6	S
O.23	12	36.0	48.4	42.4	4.1 ± 0.2	5.6	R

[a] Experimental enantiomeric purity of the starting material (ee_S) or product (ee_P).
[b] Degree of conversion calculated by using the relationship $c = ee_s/(ee_s + ee_p)$.
[c] The true enantioselectivity was calculated from ee_s and ee_p according to [21].
[d] The apparent enantioselectivity was calculated by using the colorimetric assay described in [17].

Table 3. Structure:Activity Changes in the O.16 Enzyme Caused by Chemical Treatments or Environmental Factors

Enzyme Pretreatment Conditions[a]	Physical State	Relative Hydrolase Activity	
		Esterase	Thioesterase
No pretreatment	Monomer (104 kDa)	1.0	1.0
Dithiothreitol (DTT)	Monomer (85 kDa)	—[b]	2.1
	Monomer (21 kDa)	1.9	—[b]
20–40 MPa	Trimer (325 kDa)	2.1	2.0
DTT plus 20–40 MPa	Trimer (325 kDa)	3.9	4.5
2–4 M NaCl	Trimer (325 kDa)	180.0	179.2
DTT plus 2–4 M NaCl	Trimer (325 kDa)	322.4	358.4
2–4 NaCl plus 20–40 MPa	Trimer (325 kDa)	324.0	286.7
DTT plus 2–4 M NaCl plus 20–40 MPa	Trimer (325 kDa)	720.0	715.0

[a] Samples of O.16 esterase were preincubated under different conditions, and the esterase and thioesterase activities were measured by using the standard assays. Reaction conditions: [E] = 5 μg, [substrate] = 0.8 mM for *p*-NP-esters or 4 mM for acyl-CoAs; 100 mM Tris-HCl (pH 8.5); *T* = 40°C. All values were determined in triplicate and were corrected by considering the spontaneous hydrolysis of the substrate. Results shown are the average of three independent assays. Activity values of 573 and 101 U/mg protein, corresponding to the activity showed under "*standard*" conditions, for the hydrolysis of p-NP-acetate and propionyl-CoA, respectively, were taken as 1.
[b] Hydrolytic activity not detected.

esterase gene, a 913 aa long peptide with a theoretical MW of 104,369 Da, is posttranslationally cleaved to two shorter peptide species. Under salinity and pressure conditions reflecting those of the sampling site, namely, 2–4 M NaCl and/or 40 MPa pressure, the enzyme exists as a homotrimeric protein with an apparent molecular mass of ~325 kDa (N-terminal: LNNSGYTAAQWAAI NSG). After removal of the NaCl by dialysis, or equilibration for >60 min under atmospheric pressure, the enzyme redissociated into its monomeric form; thus, the salt- and pressure-induced transitions in quaternary structure are reversible. The three different molecular species of the O.16 enzyme were purified by gel filtration chromatography, and their activities were analyzed. The essential findings are presented in Table 3 and can be summarized as follows: (1) the 325 kDa homotrimer and the 104 kDa monomer hydrolyzed *p*-NP-butyrate and propionyl-CoA, whereas the 85 kDa fragment hydrolyzed only propionyl-CoA and the 21 kDa fragment hydrolyzed only *p*-NP-butyrate; (2) the separated 85 and 21 kDa polypeptides were ca. twice as active as the 104 kDa monomer, as was the trimeric form produced by high pressure; (3) DTT plus high pressure gave a trimeric species that was 4× more active than the monomer, which indicates that the DTT-induced increase in enzyme activity does not require the complete dissociation of the 85 kDa and 21 kDa peptides; and (4) high salt-induced trimer formation was associated with a substantial increase in activity, 180× over the monomer activity, which was further increased by high pressure and DTT to a value up to 400×–700× that of the monomer. These experiments showed that the O.16 enzyme can exist in multiple active forms, generated through changes in tertiary and quaternary structures, and that more than one active site is involved in its hydrolytic activity.

Inspection of the deduced amino acid sequence revealed that the O.16 esterase showed no sequence similarity to known enzymes. However, it revealed three typical lipase/esterase motifs [16], containing putative active site serines: $GXS_{446}XG$, GDS_{807}, and $GXS_{839}XG$ (see Figure S3I). To confirm that one or more of these Ser residues participates in the catalytic activity of the enzyme, and to relate specific serines to distinct catalytic activities, single, double, and triple Ser-to-Gly mutant variants of the enzyme were generated by site-directed mutagenesis (see the Supplemental Data). Mutated proteins were expressed in *E. coli* TOP 10, purified, and assayed for esterase and thioesterase activity under standard conditions (Figure 3A). All variants, except those containing the triple mutations or the double mutations at Ser_{807} and Ser_{839}, were able to hydrolyze *p*-NP-butyrate, though less efficiently than

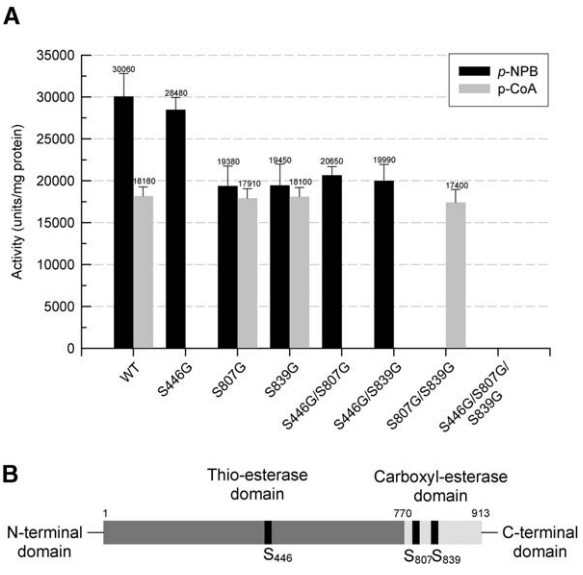

Figure 3. Activities of Mutant O.16 Esterase Variants and Primary Structure Determination

(A) Hydrolytic activity of O.16 variants with *p*-NP-butyrate (*p*-NPB) and propionyl-CoA (p-CoA) as substrates. Activity was measured by using the standard esterase and thioesterase assays. Reaction conditions: [E] = 5 μg, [substrate] = 0.8 mM for *p*-NP-esters or 4 mM for acyl-CoAs; 100 mM Tris-HCl (pH 8.5); *T* = 40°C. Bars indicate standard deviation from three different experiments

(B) Suggested primary structure of O.16 esterase. Catalytic serines are shown in bold boxes.

the wild-type protein. This suggests that both Ser residues participate in the carboxylesterase activity of the O.16 enzyme. Mutations at Ser_{446}, single or in combination, produced variants with similar activities in *p*-NP-butyrate and no activity in propionyl-CoA. All other variants exhibited thioesterase activity similar to that of the wild-type enzyme. The secondary structures of the native and mutated proteins were assessed by circular dichroism (CD). All proteins had identical CD spectra, so none of the mutations or mutation combinations detectably perturbed the folding of the thioesterase and carboxylesterase domains. These data strongly suggest (rigorous proof awaits 3D structure determination, which is in progress) that the enzyme contains three catalytic serines: Ser_{446}, located on the 85 kDa polypeptide and participating in thioesterase activity; and Ser_{807} and Ser_{839}, located on the 21 kDa polypeptide and mediating carboxylesterase (and also paraben-hydrolase; data not shown) activity (Figure 3B).

Phylogenetic Affiliations of the Mined Esterase Genes?

We have demonstrated here that esterases (and therefore presumably other enzymes, and other microbial products in general, such as lipids or secondary metabolites) with unusual properties and structures can be mined from the DHABs. An interesting issue that arises from this is the phylogenetic (and even more interesting, the physiological) novelty of the microbial origin of the new enzymes. Though it is not yet possible to make reliable protein sequence-based phylogenetic assignments of the organisms from which a protein originates, as is the case for rRNA/rDNA sequences, it may be possible to derive some phylogenetic inferences from protein sequences. We therefore made Blast searches by using the entire cloned fragments containing the esterase genes against whole microbial genomes and environmental sequences in the NCBI database, as well as against the genome sequence of *Alcanivorax borkumensis*, a marine, oil-degrading mesophilic Gammaproteobacterium [24]. We then assessed conservation of context and order of the predicted genes of the individual subfragments that gave significant alignments. A rooted amino acid tree based on an alignment of deep-sea esterases with enzymes found be homologous, using Fasta 3.3 homology searching against the UniProt protein database, is shown in Figure 4. The results of this analysis suggest that the cloned DNA fragment in O.02 (and in O.04 and, to a lesser extent, O.11) may derive from a Gram-negative bacterium (Figure S3E), probably a relative of *A. borkumensis* (the gene order in O.02 in relation to that in *A. borkumensis* is particularly well conserved). Cloned fragments in O.03, O.10, and O.12 (similar to Oil2) appear to be related (84% identity over 220 bp for O.10, 100% identity over 193 bp for O.03, and 85% identity over 220 bp for O.12) to metagenome sequences of material derived from the Sargasso Sea [25] (Figure S3B). The cloned fragment in O.23 (Figure S3G) is likely to be derived from a single-celled eukaryote. Deduced peptide sequences from cloned fragments in O.16 and O.21, which specify the most unusual esterases among the group of enzymes examined in this study, show no similarity to any putative open reading frames from DNA fragments of genome sequences in GenBank; thus, no alignments could be made. Though an inability to align cloned sequences on plasmids O.16 and O.21 with available genomes does not mean that they are derived from so far undiscovered microbes, it is consistent with the possibility of hitherto undescribed, unusual microbes with unusual properties present in DHABs.

Discussion

While DHABs are exotic, isolated habitats, their interfaces with the overlying water column have been considered by some to be simply traps for particulates descending through the water column, and thus to have biodiversity more typical of general marine habitats. In contrast, others consider such interfaces to constitute unique habitats containing unusual and highly specific life forms, with novel activities and physiologies, adapted to the specific extreme and spatially varying physicochemical conditions of the prevailing steep interfacial gradients. Our study of esterases mined from the Urania West Basin interface suggests that DHAB interfaces contain microbes and biomolecules displaying diverse functionalities that reflect life specifically adapted to the brine, to the water column, and, most interestingly, to the interface (also supported by a study of the properties of microbes cultured from the interface: see [13]). The O.02 and O.23 esterases showed relatedness to known esterases and exhibited no distinctive characteristics related to pertinent physicochemical properties of DHABs. Thus, we assume that their genes originated from bacteria that inhabit normal marine habitats and that they were either living on particulates that descended to the brine interface or were living on or close to the upper face of the chemocline. The Oil2 enzyme also showed relatedness to known esterases but exhibited halotolerance; thus, it may have originated from a brine-tolerant organism. On the other hand, the O.16 and O.21 enzymes exhibited no sequence similarity to enzymes from public databases and exhibited unusual and habitat-specific characteristics, such as preference for or tolerance of high hydrostatic pressure and salinity, and, uniquely so far, exceptional stability and activity stimulation by polar solvents. Moreover, and unlike the other esterases, they both hydrolyze thioesters. This activity is restricted to short chain thioesters, suggesting that this function lies not in fatty acid biosynthesis, the usual role of thioesterases [26], but rather in substrate scavenging in substrate-poor marine environments like DHABs. We therefore suggest that O.16 and O.21 enzymes are DHAB interface-specific, and that these interfaces are the specific habitats of the microbes that produce them. A more comprehensive survey of enzymes from the DHABs currently in progress will determine whether or not this proposal is correct.

A key question that arises is: Is the unusual functional versatility of “interface enzymes” reflected in unusual structural features? Though a definitive description of the structural features of the O.16 and O.21 enzymes awaits elucidation of their 3D structures, the O.16 enzyme clearly exhibits, to our knowledge, unique char-

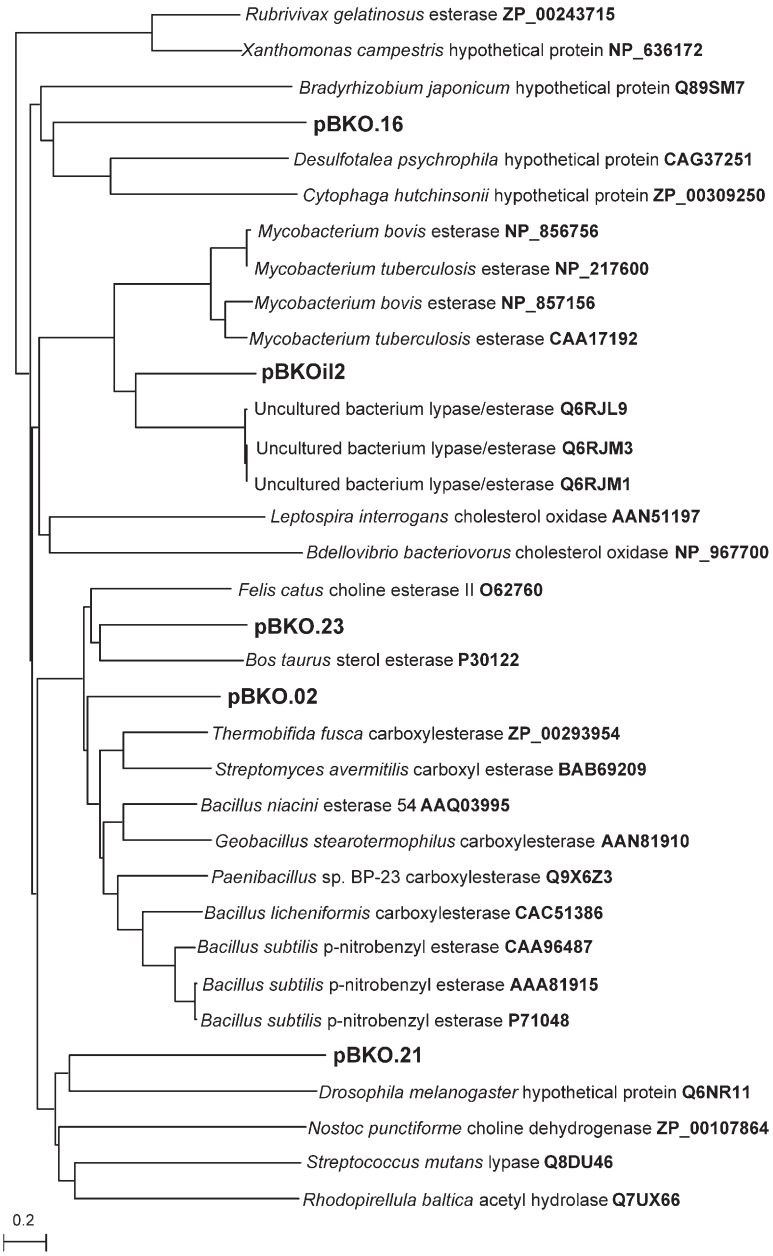

Figure 4. Rooted Phylogenetic Tree Based on the Alignment of DHAB Esterases

Rooted amino acid tree based on an alignment of deep-sea esterases (shown in bold) with enzymes found to be homologous by using Fasta 3.3 homology searching against the UniProt protein database (release 2.3; 1,536,117 entries) with the BLOSUM50 matrix. Multiple sequence alignment was constructed by using MacVector 7.2.2 software (Accelrys, San Diego, CA) with the BLOSUM matrix; open and extend gap penalties of 10.0 and 0.05, respectively. The alignment file was then analyzed with the same software for calculation of the distance matrix. Neighbor Joining and Poisson correction of distances were used to construct the phylogenetic tree. *Mus musculus* nuclear receptor subfamily 3, group C, member 2 (Q8VII8) was used for tree rooting. The bar represents 2.0 changes per amino acid.

acteristics: first, it represents the largest esterase known (325 kDa versus 210 kDa for the *Aureobasidium pullulans* feruroyl esterase); second, it possesses a substantially higher level of structural complexity than known esterases, incorporating three catalytic active centers, one located in a 770 aa long peptide harboring the thioesterase activity, and two located in a 198 aa long peptide having the carboxylesterase activity. This feature is so far unique in esterases: although sequence inspections of some lipases have revealed two potential catalytic serines, functional analyses have demonstrated only one to be involved in catalysis [27, 28]. Thus, the O.16 enzyme has a higher level of structural complexity than any known esterase. Even more interesting are the changes in structure of the O.16 enzyme in response to changes in physicochemical conditions pertinent to the Urania Basin interface. Under the conditions of low salinity and hydrostatic pressure that characterize the upper water column, the enzyme will exhibit a bifunctional monomeric structure with high catalytic activities for both types of substrates. Under the conditions of hydrostatic pressure prevailing at lower depths in the water column, and at the seawater:brine interface, however, monomer subunits are expected to reversibly associate to form a bifunctional trimeric species having even higher catalytic activities. In the interface, where the concentration of NaCl rapidly increases to ca. 4 M, the activity should sharply increase by more than two orders of magnitude. And, under anoxic, and thus reducing, conditions of the body brine, the enzyme should experience a further increase in activity. These features of the O.16 enzyme

suggest a remarkable adaptive structure:function configuration that may have evolved to assure catalytically powerful functionalities over the wide range of physicochemical conditions prevailing in the marine water column, the steep gradients of physicochemical conditions at seawater:brine interfaces of DHABs, and the highly stressful extreme conditions of DHAB brines.

An important consequence of this work is the identification of five carboxylesterases from an extreme biotope that are potent biocatalysts for the synthesis of optically pure compounds and certain pharmaceutical intermediates [29]. Two of the five mined esterases have no relatives in any current database, three are characterized by high ratios of hydrolytic rates (calculated in μmol/s per μmol protein) varying from 3064 to 3462, and four exhibit high enantioselectivities toward industrially relevant chemicals. The O.16 enzyme has the highest enantioselectivity value described so far for the hydrolysis of esters of the important chiral synthon solketal (*E*: 126; optical purity: >98%*ee*, [S]-form), which is considered to be an important intermediate for therapeutic drug development, e.g., for AIDS [19, 20]. Furthermore, the O.16 and O.21 esterases were found to hydrolyze and also to catalyze a transesterification reaction of esters of *p*-hydroxybenzoic acid (parabens) and of α amino acid esters, respectively. Both substrates and their derivatives (i.e., β-lactam antibiotics) are important conservation agents in the pharmaceutical, cosmetic, and food industries. All esterases displayed optimal activities at pH 8.0–9.0 and 40°C–60°C, which are the conditions routinely used in chemical synthesis processes. Of particular interest is the so far unusual tolerance of some of these enzymes, particularly the O.16 esterase, to extremes of pressure, pH, salts, and especially to polar solvents, agents that rapidly inactivate most esterases and lipases. This tolerance is a highly advantageous property for many organic syntheses.

Significance

We have demonstrated that the activity-based mining of "metagenome" libraries of microbial genetic resources from unusual and extreme environments results in the discovery of remarkable enzymes. As far as we know, esterases mined from the metagenome library of the Mediterranean Urania Basin hypersaline brine interface have unusual structures and superior catalytic properties to other known esterases, and they therefore may be candidates for the synthesis of optically pure compounds and pharmaceutical intermediates. If, as we suggest here, these esterases serve as proxies of other enzymes and metabolic activities of the microbes of the DHABs, then a significant amount of new diversity is waiting to be discovered in such brines and their interfaces.

Experimental Procedures

Full details of all experimental methods are given in the Supplemental Data.

Strains and Buffers

Restriction and modifying enzymes were from New England Biolabs (Beverly, Massachusetts). *E. coli* strains XL1-Blue MRF' for library construction and screening and XLOLR for expression of the esterases from phagemids (Stratagene; La Jolla, California) and TOP 10 for site-directed mutagenesis and expression of mutant esterases (Invitrogen; Carlsbad, California) were maintained and cultivated according to the recommendations of suppliers and standard protocols described elsewhere [30]. Unless mentioned otherwise, the standard buffer used in the present study was 100 mM Tris-HCl buffer (pH 8.5).

Construction of Environmental DNA Libraries and Screening for Genes Conferring Esterase Activities

Brine interface samples from the Urania West Basin of the Mediterranean Sea (35°13′51′′N; 21°28′24′′E; 3552 m depth) were taken during the BIODEEP-II cruise of the RV *Urania* (September, 2001) with the instrumented module SCIPACK, specifically developed to enter into the brines and to take measurements and samples in an accurate and controlled way. Once raised to the surface and on board, the entire volume of one Niskin bottle (2 L) was immediately transferred aseptically to a Widdel bottle containing an atmosphere of sterile N_2/CO_2 (4/1). A 20 ml subsample was immediately transferred to a 100 ml culture flask preflushed with the same gas mixture and containing sterile crude oil (Arabian light, 0.5% [vol/vol]) to stimulate microbial growth and increase biomass. After 4 weeks of incubation at 15°C, total DNA was extracted from the culture by means of a G'NOME extraction kit (Qbiogene; Carlsbad, California), and a metagenome expression library in the bacteriophage lambda-based ZAP phagemid vector (ZAP Express Kit, Stratagene) was constructed as described in the manufacturer's protocols. A library of 4×10^8 phage particles, with an average insert size of about 5 kbp, was thereby generated. Phage particles were used to infect *E. coli* XL1-Blue MRF' cells, which were subsequently plated on 22.5 × 22.5 cm square plates to give approximately 7000 phage plaques per plate. After overnight incubation, the plates were overlaid with 20 ml of a water solution containing 320 μl α-naphtyl acetate (20 mg/ml in dimethylsulfoxide), 5 mM IPTG, and 320 μl Fast Blue RR (80 mg/ml in dimethylsulfoxide). Esterase-positive plaques exhibiting a brown halo after 30–120 s were picked, and clones were purified by dilution and replating. Phagemids were subsequently generated from pure clones by coinfection with helper phage, as described in the Stratagene protocols, isolated, and analyzed by restriction enzyme digestion. Cloned inserts of plasmids specifying esterases were completely sequenced, initially from both ends, by means of universal primers, and subsequently by primer walking. Further details for cloning and expression and purification procedures of esterases are provided in the Supplemental Data.

Phylogenetic Tree Construction

Multiple sequence alignments were made with the ClustalW online tool for the protein sequences. The conserved motifs in the image, which classify them in respective families, are highlighted. Closely related homologs were identified from a NCBI nonredundant database by conducting BLAST searches. Sequences with alignment >50% (over the length of the protein) and an e value better than e^{-08} (for Oil2 and related), e^{-33} (for O.02), and e^{-28} (for O.23) were considered. From these hits, a multiple sequence alignment file was constructed with the CLUSTALW online tool. The alignment file was then analyzed with PROTDIST of the PHYLIP package for calculation of distance matrix. NEIGHBOR (PHYLIP3.61) was used to construct the phylogenetic tree by using a neighbor joining method by following the Dayhoff PAM matrix model. The topology shown is a consensus neighbor joining tree obtained after 100 bootstrap replicates. Bootstrap values >60% are shown. The tree was visualized by using TREEEXPLORER software. The possible catalytic triad (Serine [S], Aspartic acid [D], Histidine [H]) is shown at the top of the alignment whenever necessary.

Supplemental Data

Supplemental Data including additional Experimental Procedures, tables (Tables S1–S5), and figures (Figures S1–S6) are available at http://www.chembiol.com/cgi/content/full/12/8/895/DC1/.

Acknowledgments

M.F. thanks the European Commission for a Marie Curie postdoctoral fellowship and the Spanish Ministerio de Ciencia y Tecnología. This research was supported by European Community Projects EVK3-2000-00042 "BIODEEP," EVK3-2002-00077 "COMMODE," and MERG-CT-2004-505242 "BIOMELI." The authors acknowledge the "GenoMik" initiative of the German Federal Ministry of Science and Education (BMBF). K.N.T. gratefully acknowledges generous support by the Fonds der Chemischen Industrie. We also thank Rita Getzlaff for protein sequence analyses and Francisco J. Plou, Nieves López, and Dolores Reyes for their technical assistance in esterase activity measurements. We also thank other members of the BIODEEP consortium for their intellectual and technical support and the pleasure of their company on this expedition of discovery. We especially acknowledge the crew of research vessel RV *Urania* for excellent assistance and winch operation during interface samplings.

Received: February 4, 2005
Revised: May 5, 2005
Accepted: May 31, 2005
Published: August 26, 2005

References

1. Amaral Zettler, L.A., Gomez, F., Zettler, E., Keenan, B.G., Amils, R., and Sogin, M.L. (2002). Microbiology: eukaryotic diversity in Spain's River of Fire. Nature *417*, 137.
2. Torsvik, V., and Ovreas, L. (2002). Microbial diversity and function in soil: from genes ecosystems. Curr. Opin. Microbiol. *5*, 240–245.
3. Hewitt, G.M. (2004). The structure of biodiversity-insight from molecular phylogeography. Front. Zool. *1*, 4.
4. Ciaramella, M., Napoli, A., and Rossi, M. (2005). Another extreme genome: how to live at pH 0. Trends Microbiol. *13*, 49–51.
5. Dolan, J.R. (2005). Marine ecology: different measures of biodiversity. Nature *433*, E9.
6. Whitman, W.B., Coleman, D.C., and Wiebe, W.J. (1998). Prokaryotes: the unseen majority. Proc. Natl. Acad. Sci. USA *95*, 6578–6583.
7. Koonin, E.V., Wolf, Y.I., and Karen, G.P. (2002). The structure of the protein universe and genome evolution. Nature *420*, 218–223.
8. Handselman, J., Rondon, M.R., Brady, S.F., Clardy, J., and Goodman, R.M. (1998). Molecular biological access to the chemistry of unknown soil microbes: a new frontier for natural products. Chem. Biol. *5*, 245–249.
9. Streit, W.R., and Schmitz, R.A. (2004). Metagenomics—the key to the uncultured microbes. Curr. Opin. Microbiol. *7*, 492–498.
10. Vengosh, A., and Starinsky, A. (1993). Relics of evaporated sea water in deep basins of the eastern Mediterranean. A. Mar. Geol. *115*, 15–19.
11. Aloisi, G., Pierre, C., Della Vedova, B., and Corselli, C. (2001). Carbon isotope measurements in the brines of the Urania and l'atalante anoxic basins, eastern mediterranean. Archo. Oceanogr. Limnol. *22*, 87–90.
12. Sass, A.M., Sass, H., Coolen, M.J., Cypionka, H., and Overmann, J. (2001). Microbial communities in the chemocline of a hypersaline deep-sea basin (Urania basin, Mediterranean Sea). Appl. Environ. Microbiol. *67*, 5392–5402.
13. van der Wielen, P.W., Bolhuis, H., Borin, S., Daffonchio, D., Corselli, C., Giuliano, L., D'Auria, G., de Lange, G.J., Huebner, A., Varnavas, S.P., et al. (2005). The enigma of prokaryotic life in deep hypersaline anoxic basins. Science *307*, 121–123.
14. Wallmann, K., Aghib, F.S., Castradori, D., Cita, M.B., Suess, E., Greinert, J., and Rickert, D. (2002). Sedimentation and formation of secondary minerals in the hypersaline Discovery Basin, eastern Mediterranean. Mar. Geol. *186*, 9–28.
15. Hübner, A., De Lange, G.J., Ditter, J., and Halbach, P. (2003). Geochemistry of an exotic sediment layer above sapropel S-1: mud expulsion from the Urania Basin, eastern Mediterranean? Mar. Geol. *197*, 49–61.
16. Arpigny, J.L., and Jaeger, K.-E. (1999). Bacterial lipolytic enzymes: classification and properties. Biochem. J. *343*, 77–183.
17. Khmelnitsky, Y.L., and Rich, J.O. (1999). Biocatalysis in nonaqueous solvents. Curr. Opin. Chem. Biol. *3*, 47–53.
18. Powers, J. (1997). Reaction of serine proteases with halomethyl ketones. Methods Enzymol. *46*, 197–208.
19. Janes, L.E., Löwendahl, C., and Kazlauskas, R.J. (1998). Rapid quantitative screening of hydrolases using pH indicators. Finding enantioselective hydrolases. Chem. Eur. J. *4*, 2317–2324.
20. Bornscheuer, U.T. (2004). High-throughput-screening systems for hydrolases. Eng. Life Sci. *4*, 539–542.
21. Lorenz, P., Beton, K., Niehaus, F., and Eck, J. (2002). Screening for novel enzymes for biocatalytic processes: accessing the metagenome as a resource of novel functional sequence space. Curr. Opin. Biotechnol. *13*, 572–577.
22. Weissfloch, A.N.E., and Kazlauskas, R.J. (1995). Enantiopreference of lipase from *Pseudomonas cepacia* toward primary alcohols. J. Org. Chem. *60*, 6959–6969.
23. Chen, C.S., Fujimoto, Y., Girdaukas, G., and Sih, C.J. (1982). Quantitative analysis of biochemical kinetic resolutions of enantiomers. J. Am. Chem. Soc. *104*, 7294–7299.
24. Golyshin, P.N., Martins Dos Santos, V.A., Kaiser, O., Ferrer, M., Sabirova, Y.S., Lünsdorf, H., Chernikova, T.N., Golyshina, O.V., Yakimov, M.M., Puhler, A., et al. (2003). Genome sequence completed of *Alcanivorax borkumensis*, a hydrocarbon-degrading bacterium that plays a global role in oil removal from marine systems. J. Biotechnol. *106*, 215–220.
25. Venter, J.C., Remington, K., Heidelberg, J.F., Halpern, A.L., Rusch, D., Eisen, J.A., Wu, D., Paulsen, I., Nelson, K.E., Nelson, W., et al. (2004). Environmental genome shotgun sequencing of the Sargasso Sea. Science *304*, 66–74.
26. Holmquist, M. (2000). Alpha/beta-hydrolase fold enzymes: structures, fun and mechanisms. Curr. Protein Pept. Sci. *1*, 209–235.
27. Brok, R.G., Belandia, I.U., Dekker, N., Tommassen, J., and Verheij, H. (1996). *Escherichia coli* outer membrane phospholipase A: role of two serines in enzymatic activity. Biochemistry *18*, 7787–7793.
28. Sheriff, S., Du, S., and Grabowski, G.A. (1995). Characterization of lysosomal acid lipase by site-directed mutagenesis and heterologous expression. J. Biol. Chem. *270*, 27766–27772.
29. Koeller, K.M., and Wong, C.-H. (2001). Enzymes for chemical synthesis. Nature *409*, 232–240.
30. Sambrook, J., Fritsch, E.F., and Maniatis, T. (1989). Molecular Cloning: A Laboratory Manual, Second Edition (Cold Spring Harbor, NY: Cold Spring Harbor Laboratory Press).
31. Schlitzer, R. (2003). Ocean Data View (http://awi-bremerhaven.de/GEO/ODV).

Accession Numbers

Mined genes coding for esterases and polypeptide sequences translated from these have been submitted to the EMBL/DDBJ/GenBank databases under accession numbers AJ811965 (Oil2), AJ811966 (O.02), AJ811967 (Oil16), AJ811968 (O.21), and AJ811969 (O.23). Accession numbers of sequences used in this study are given in Table S5.